17th World Conference on Earthquake Engineering, 17WCEE

Sendai, Japan - September 13th to 18th 2020

EVALUATING STATE-OF-THE-ART METHODOLOGIES FOR POST-EARTHQUAKE STRUCTURAL RECONNAISSANCE

M. Mostafa[(1)], L. Hogan[(2)], M. Stephens[(3)] , M. Olsen[(4)] , K. Elwood[(5)]

[(1)] *ME Student, University of Auckland, mmos855@aucklanduni.ac.nz*
[(2)] *Lecturer, University of Auckland, lucas.hogan@auckland.ac.nz*
[(3)] *Lecturer, University of Auckland, max.stephens@aucklad.ac.nz*
[(4)] *Professor, Oregon State University, michael.olsen@oregonstate.edu*
[(5)] *Professor, University of Auckland, k.elwood@auckland.ac.nz*

Abstract

Following an earthquake, there is a need to rapidly collect perishable data to evaluate the seismic performance of structures and aid in decision making regarding structural integrity and safety. Traditional reconnaissance methods, such as visual inspection and photographing of damage by individual researchers, can be time consuming and dangerous, particularly during periods of heightened aftershock activity. These reconnaissance methods are also limited in their effectiveness, as there are often gaps in damage documentation and visual records, resulting in challenges to correlate reconnaissance data with other layers of information such as instrumentation records or structural models. Newer reconnaissance techniques, such as terrestrial laser scanning, structure from motion\multi-view stereo (SfM\MVS) photogrammetry, and unmanned aerial systems photography/videography, hold substantial promise to mitigate the aforementioned shortcomings of traditional post-earthquake reconnaissance methods. However, to date, these technologies have been minimally exploited relative to their potential. This paper explores the capabilities and limitations of these technologies with application to a case study consisting of a reinforced concrete building with precast concrete floors damaged during the 2016 Kaikoura New Zealand Earthquake. The structure was extensively surveyed using several state-of-the-art methodologies to document the severity and distribution of damage resulting from the earthquake. Key factors that influenced the quality of data gathered are discussed along with limitations discovered for the utilized methods. Finally, procedures and challenges to combine data to create a detailed 3D model from the different survey methods (e.g. 3D laser scans and SfM/MVS) are presented. This model provides detailed damage documentation with limited visual gaps and can be used in conjunction with other layers of reconnaissance data to aid in the validation of detailed structural analysis models. The presented work shows that terrestrial laser scanning and SfM\MVS have significant merit for capturing structural damage when compared to traditional methods. At the level of detail of the surveys completed, these techniques successfully captured cracks with widths less than 1 mm using SfM\MVS and cracks with widths of approximately 2 mm using high-resolution terrestrial laser scanners, allowing for 3D visualization of structural damage that cannot be seen using conventional means, providing the chance for better understanding of structural performance and proves its ability to aid in decision-making post an earthquake event.

Keywords: Post-earthquake reconnaissance; 3D damage documentation; Laser scanning; Structure from motion

1. Introduction

Reconnaissance surveys following strong earthquakes provide valuable insight into damage and structural performance, which allows engineers to improve design standards and building codes that can lead to more resilient structures [1]. Traditionally, visual inspection has been the primary technique for post-earthquake field surveying for the assessment of structural damage and performance. However, reliance on visual inspections is time-consuming and introduces uncertainty and subjective opinion into the assessment. The subjectivity of visual inspection is often exacerbated by limited accessibility to damaged parts of structures and time constraints which lead to gaps in damage documentation and visual records. This time pressure is particularly acute for structural reconnaissance to avoid interfering with rescue, relief and repair efforts. Therefore, more advanced techniques are required to improve overall standards of inspection and documentation whilst minimizing the time required to complete the inspection. One advancement which has recently been implemented in post-earthquake reconnaissance is the use of terrestrial laser scanning (TLS). TLS technology (also known as Light Detection and Ranging, lidar) is rapidly gaining attention in many fields as it captures millions of data points from the subject structure with resolution and accuracy down to several millimetres. Lidar for post-earthquake reconnaissance can either be deployed on an airborne or terrestrial platform. Aerial lidar has been utilized previously in reconnaissance efforts, where a scanner was mounted on an aircraft that flies over the affected area to capture data. Aerial lidar has typically been used for large scale reconnaissance such as fault mapping and generating slope maps [2], but has not been used extensively for structural reconnaissance given that the data are generally not of sufficient accuracy and resolution. Terrestrial laser scanners have not been used as widely in reconnaissance efforts due to the several factors that include inaccessibility to damaged structures and the limited coverage of TLS relative to aerial lidar [3]. The limited use that TLS have had in post-earthquake structural reconnaissance missions has been focused on global structure level surveys rather than structural element level investigation [4].

One early deployment of terrestrial lidar for post-earthquake reconnaissance occurred following the 2004 Niigata earthquake [5]. The reconnaissance team utilized TLS to create high-resolution, three-dimensional, virtual models of earthquake-related ground, structural, and lifeline deformations. TLS allowed field researchers to collect data for a large geographic area that included areas that were inaccessible by foot, unstable, and/or dangerous to access. Data collected using the TLS enabled engineers to measure structural deformation accurately (e.g., slab deformation) in a matter of minutes for work area that would have taken hours or days to measure using traditional methods [6]. Other early utilizations of TLS include Mosalam et al. [4] and Olsen et al. [7] for large scale damage surveys of the 2010 Haiti and 2010 Maule earthquakes, respectively. Both of these studies scanned multiple structures, which were compared to qualitative results obtained from visual ground survey. While these previous studies demonstrated the ability of TLS to rapidly collect data over a large area and detect information difficult to observe using traditional reconnaissance techniques, there are a limited number of case studies utilizing TLS for post-earthquake damage assessments, particularly focusing on specific structural elements and components. Additionally, few studies evaluate the data quality of these sensors in context of post-earthquake reconnaissance, resulting in limited guidance as to their capabilities and limitations.

This paper explores the capabilities and limitations of TLS and high-resolution imagery processed using close-range terrestrial structure-from-motion\multi-view stereo (SFM\MVS) for detailed post-earthquake reconnaissance which focuses on damage to structural elements within a single building. High-resolution 3D data was collected and used to generate a model of a case study reinforced concrete building with precast concrete floors damaged during the 2016 Kaikōura earthquake. The structure was surveyed using two different laser scanners as well as a high-resolution camera that generated a 3D SFM\MVS model for zones with heavy damage to document the severity and distribution of damage resulting from the earthquake. The capabilities and limitations of each technique are compared and discussed to provide valuable insight into using these technologies for future reconnaissance missions.

2. Case study overview

The magnitude 7.8 Kaikōura earthquake occurred along the east coast of the upper South Island of New Zealand on 14 November 2016. The event ruptured multiple fault segments and generally propagated northward from Kaikōura into the Wellington region [8]. The characteristics of the ground motion in Wellington resulted in shaking in excess of design level demands for buildings in the one to two second period range at some locations within Wellington [9], including the case-study building evaluated in this research.

The layout of the case-study building was unique, consisting of three seismically linked piers each of five to six floors (refer to Figs. 1 and 3). The principal lateral load system in each pier consisted of reinforced concrete moment frames in both directions, and a diaphragm of precast hollow-core floor units with in-situ topping. The building was evaluated using three data collection techniques with the objective of evaluating the capabilities and limitations of each technique. Two different TLS systems with different accuracy and range specifications were used to investigate the capability of different scanners to detect structural damage through point cloud data and spherical camera images. Close-range SFM/MVS photography was also used in areas of high interest (e.g. beam-column joints).

2.1 Reconnaissance equipment

The reconnaissance equipment used in this study consisted of two TLS systems with different capabilities as well as high resolution cameras for close-range SFM. As structural reconnaissance of the case study building was performed from inside the building, short-range laser scanners were selected. Two TLS's with different capabilities, representing a low-cost and a medium-cost scanner, were selected to allow for a comparison of the relative performance of each system in capturing structural damage. Namely, a Leica BLK 360 representing the low-cost scanner and a Leica RTC 360 representing the medium-cost scanner with relatively higher accuracy. Both scanners used high speed time-of-flight-based ranging enhanced by Waveform Digitizing (WFD), where the duration of the light travel is measured and used in the estimation of the coordinates of each point on the object relative to the scanner location. Both scanners also interpret the intensity of the reflected light, which is a function of material and colour, but also impacted by range and the angle of incidence. Both scanners also have built in cameras to apply RGB colours to the resulting point cloud produced through the scanning process to digitally map the scene. The accuracy of the model generated depends on several factors, some of them include the scanner resolution, both scanners have three resolution levels to choose from (high, medium and low), and the distance between the scanner and the object [10]. The specifications of the two scanner types used are summarized in Table 1.

In addition to the two TLS, a high-resolution Nikon D5600 camera with 24.2 effective megapixels and ISO range 100-25600 was used for close-range SFM\MVS. SFM\MVS is a technique that generates a 3D structure of an object from a set of 2D images, and maps the images into a cohesive model using an object recognition system or algorithm that utilizes local image features. This technique is used to create high-resolution digital surface models and models of objects using digital cameras. SFM/MVS also produces a 3D point cloud model similar to the point cloud generated using lidar. The accuracy and level of detail of the 3D point cloud depends on the quality of the 2D images (including the amount of overlap in the 2D images) and the processing algorithm. Here, a lens with a 10 mm fixed focal length was used, as performing close-range SFM/MVS in this relatively tight space required a wide lens to capture greater area to insure achieving the required overlap.

Table 1- Scanners specifications

	Leica RTC360	**Leica BLK360**
General	High-speed 3D laser scanner with integrated HDR spherical imaging system	3D scanner with integrated spherical imaging system and thermography panorama sensor system
Range	130 m	60 m
Scan rate	2,000,000 point per second (max)	360,000 point per second (max)
High resolution scan	3 mm at 10 m	5 mm at 10 m
Medium resolution scan	6 mm at 10 m	10 mm at 10 m
Low resolution scan	12 mm at 10 m	20mm at 10 m
Data acquisition	< 2 minutes for complete full dome scan and spherical HDR image at standard (medium) resolution	< 3 min for complete full dome scan, spherical image & thermal image at standard (medium) resolution
Imaging	36 megapixels 3-camera system, captures 432 MPx raw data for calibrated 360° x 300° spherical image	15 megapixels 3-camera system, 150 MPx full dome capture, HDR, calibrated spherical image, 360° x 300°

2.2 Scan locations and sampling methods

Prior to scanning, a walkthrough of the building was conducted to (1) select scan locations, (2) place scanning targets and (3) highlight damage in selected locations. The scan locations were selected to optimize the number of scans and minimize the time required on-site. During the walkthrough, critical regions with concentrated damage were identified via visual inspection to ensure these regions would be adequately captured by the scans. Here, the critical regions included damage to beams and columns at beam-column joints, and damage to precast slabs at the intersection of the precast slabs and the beam-column joints. To adequately capture the damage in these critical areas, scan locations were primarily focused around the columns as illustrated in Fig. 1. To obtain full coverage of each floor and assist with registering point clouds between the scanners around the columns, a series of scans were additionally acquired from the middle of the floor span as shown in Fig.1. After the scan locations were selected, they were marked on the floor to facilitate efficiency during scanning.

Next, scanning target locations were selected and scanning targets were applied so that data collected from multiple scans (either for a single scanner or for combining the TLS and SFM/MVS 3D scan data) could be registered and combined into a cohesive model. The 90 mm x 120 mm targets were placed at the top and bottom of each column face and consisted of black and white boxes pattern as shown in Fig. 2.

Finally, damage in the structure was highlighted in select locations. Specifically, cracks were mapped on the diaphragm, soffit of the floor above and columns and beams in Piers 2 and 3as shown in Fig. 2. The cracks on the diaphragm were measured manually for comparison with the crack width identified using the different scanning methods. Cracks in Pier 1 were not marked to determine the ability of the damage detection techniques to identify cracking without pre-mapping.

A total of 873 scans were performed throughout the case-study building. A total of 515 scans were performed using the low-cost (BLK360) scanners over a period of approximately two full working days, covering a total area of almost 11,565 m^2. Three BLK scanners were used simultaneously with two personnel moving the scanners. Each scan required approximately four minutes to complete at standard resolution. To facilitate the registration process, each scan was identified by its exact time and date and marked on a sketch of the building plan. The data collected was saved on a built-in internal storage.

Using the higher accuracy scanner (RTC360) a total of 358 scans were performed over a period of approximately two working days using a single scanner, covering a total area of almost 13,875 m^2. In addition to interior scans, nineteen exterior scans were completed using the RTC scanner to capture the entire structure as shown in Fig. 3. The RTC scanner was operated by a single person, a second person was required to be there for safety reasons, and each scan required approximately three minutes to complete. Utilizing the ability of the scanner to track its movement and position relative to the previous setup in real time, on-site initial registration was done, saving substantial post-processing time. The scanner's main storage is on a portable USB drive inserted into the scanner, where scans were directly saved on the USB drive to facilitate data transfer.

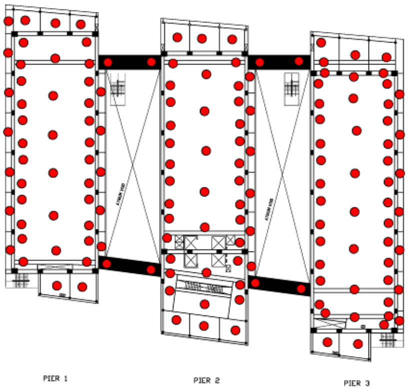

Fig. 1- Scans locations on building plan for each floor.

Fig. 2- Targets locations on top and bottom of each face of columns

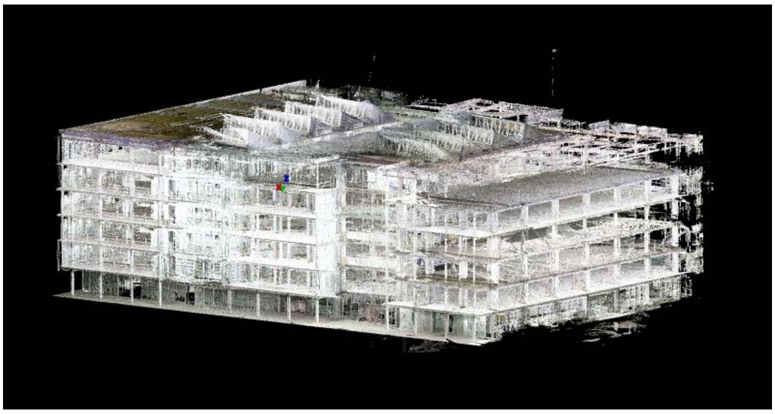

Fig. 3- Registered scans of the building

In the critical regions of the structure, close-range SFM/MVS models were developed to capture more details in those areas of interest. As identified above, these regions included beam-column joints and the intersection of the precast slabs and the beam-column joints both on the ceiling and floor of each level. Images were collected with a minimum of 70% overlap coverage on all sides to ensure there were a sufficient number of common features in adjacent images for the generation of the 3D model. All images were taken from a fixed distance from the elements being photographed to attempt to obtain a uniform coverage while maximizing overlap. An average of 68 (6000 x 4000 pixels) images was taken for each column at twelve different locations with six different elevation angles around the column. Each floor took approximately one and half to two hours to collect images for each column.

One of the challenges when collecting images for the SFM/MVS was the different lighting conditions on columns in the exterior frames. Prior work has shown that different light exposure across a single element can affect the quality of the 3D model generated from SFM/MVS [11]. Here, two distinct exposures were noted on the external columns, namely a bright exposure on the external face from sun light and a dark exposure on the internal face due to a lack of natural lighting. An attempt to balance the light exposure using portable lights in different locations around column regions was explored part of this case study.

2.3 Post-processing

To develop useful models from the scanning data and photographs, all data was extracted and post-processed. Before extracting information from the scanning data, point clouds from each scan were registered together to create a single point-cloud for the entire building. Point cloud registration was performed using Leica Cyclone Register 360 as it provides an easy work flow and then imported to Cyclone Register[12], which allows for extensive manipulation and management of point clouds and scan data. Data collected from the BLK scanners were imported into the software, where data transfer relied on Wi-Fi connection between the scanner and the computer, as no cable transfer was available. Transferring the data collected from the scanners took approximately one week. Then manual visual alignment registration for scans was performed and the point cloud model was cleaned by removing noise points. Noise points occurred mainly due to reflective surfaces such as windows that reflected points in wrong positions. After the data was cleaned, the scan registration was globally optimized to generate the best overall fit, and the data density was optimized by down sampling to an acceptable density and the data was filtered to analyse different sections reducing computational demand for more efficient data manipulation. The same procedure was used for the RTC scans except for data transfer and manual registration. Because the data were saved on a USB drive, data transfer was done by simply removing the USB drive from the scanner and plugging it into the computer with data transfer occurring within hours. Furthermore, initial registration was automatically completed by the scanner on-site during scanning. For crack mapping, optimized point clouds were exported to another software, Cloud-Compare [13], to further manipulate the cloud such that the crack detection capabilities of both scanners could be investigated.

For the close-range SFM, high resolution images were used to process a 3D model using Autodesk Recap Photo [14]. Adjustments in exposure were made to the images taken at the perimeter columns to improve the mesh quality in the 3D model. Once the model had been generated by the software, noise from the surroundings of the element being scanned was removed, and dimensions generated by the model were measured and compared to the actual measurements obtained from the structural drawings for scaling. And the final model was then exported as a point cloud for analysis.

3. Capabilities and limitations of reconnaissance techniques used

3.1 Laser Scanning

The ability of TLS's to capture millions of points from the object scanned with accuracies of few millimetres provides dense range measurement data to model an object in 3D. Utilizing its abilities, the application of TLS in post-earthquake field survey for structural damage detection was investigated, where the ability to capture damage as well as the efficiency with which the data was collected and post-processed were explored. In terms of data collection, TLS's are not sensitive to lighting conditions and can capture large amounts of accurate field data in a short period of time. Both of these features allow TLS to be deployed successfully in a wide range of environmental conditions post an earthquake event. The insensitivity to light was a significant advantage in the building, in which exposure conditions changed significantly from the perimeter of the building to the unlighted interior. By not needing portable lighting, the scans were able to be achieved more rapidly and with less personnel, making TLS a more attractive reconnaissance technique when aftershock activity is likely or other time critical scenarios are present. In terms of data outputs, the point cloud was able to provide detailed information about structural performance and damage. For example, point cloud data was used to plot vertical floor deformation as shown in Fig. 4, where it can be seen that local depressions occurred on the floor in between frame bays. It was determined that data from the point cloud can be used to identify cracks with widths within the range of 1-2 mm as shown in Fig. 5.

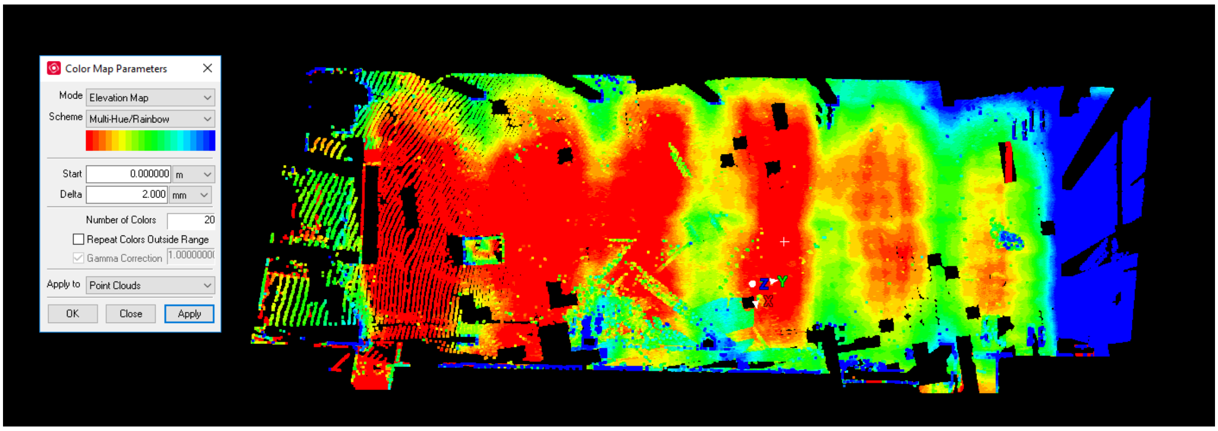

Fig. 4- Example of floor deformation using a colour map with an order of 2 mm difference - Pier1-Floor2

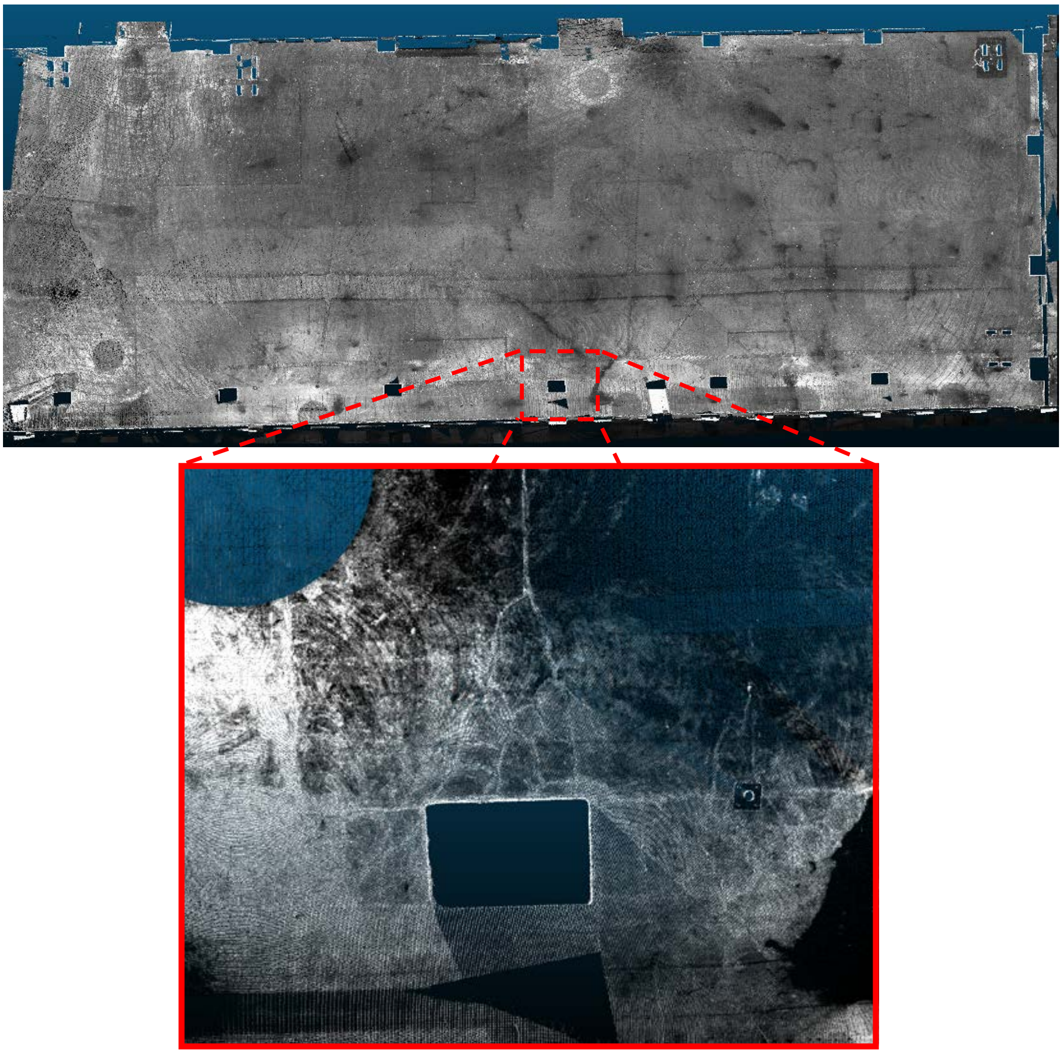

Fig. 5- Example of floor cracking detected by TLS– Pier3-Floor2

3.1.1 Multiple low-cost scanners

Some of the advantages of the low-cost scanner included the ease of operation and portability, as the scanner is light in weight (1 kg). This portability is an important consideration when selecting the equipment to be used in a post-earthquake environment. Also, what made the scanner handling easy was the operation of the scanner, where scanning settings were pre-set so the scanners could be moved and captured efficiently without adjusting settings. This turnkey operation meant that non-expert members of the reconnaissance team could be trained on the use of the scanners in a matter of minutes. One of the key factors that affected the quality of data captured was the time available to capture data on-site. The use of the highest resolution available, reaching 5-6 mm at 10 m distance, took approximately 5 minutes per scan. While this resolution would have quadrupled the point cloud resolution, it would have increased the time-on-site by one to two days. Due to the large number of close-range scans to the columns, a medium resolution scan that took approximately 3 minutes per scan was used to capture the damage sustained in the building with the required level of details within the available time window. Using the standard resolution scans from approximately 2 meters apart from the region of interest 2 mm cracks were detected. Another significant limitation that was found included data storage and transfer, where the data captured was stored locally on each device and the main method of data transfer relied on Wi-fi connection, making the transfer process extremely slow. For this case study, as three scanners were used to cover the building the batteries were changed once per day while collecting data on-site.

3.1.2 Single medium-cost scanner

One of the main advantages of the medium-cost scanner was its ability to automatically detect the location of the scanner relative to previous scans, making the scans registration easier and saving a considerable amount of post-processing time. Also, the time required per scan was similar to that used in the low-cost scanner, approximately 3 minutes, even using the highest scan resolution available, 3 mm at 10 m distance. Due to this higher scan resolution, 2 mm cracks were clearly visible, and cracks down to 0.65 mm were still detectable. Another advantage was data storage and transfer, where data could be stored and transferred using external memory.

3.2 Structure-from-motion

Close-range SFM/MVS has several advantages and disadvantages relative to TLS. SFM/MVS is generally more cost efficient than TLS, as only a high-resolution camera is necessary for data collection, and most reconnaissance teams already have such a camera available. In addition, SFM/MVS is more efficient during post-processing, as creation of the 3D model doesn't require manual processing and requires minimal post-processing work. While the manual processing is limited in SFM, the generation of the 3D model and point cloud can become computationally intensive. Also, an important consideration that is often overlooked is that SFM/MVS requires measurements (e.g., survey control, tape etc.) to provide scale for the model generated, which results in additional time. SFM/MVS is also extremely sensitive to lighting conditions, with variations in light intensity and exposure largely influencing the quality of the 3D models. An example of a 3D model generated with poor lighting conditions is shown in Fig. 6. In this case, hole developed in the model due to variations in exposure around the column, resulting in a loss of data in those locations. In addition, close-range SFM/MVS is sensitive to the distance from which the photographs are taken from the object. Special care must be taken to ensure the images are taken equidistant from the object, or the quality of the 3D image may be compromised. This shortcoming can become rather severe in cases where access is limited. Finally, SFM/MVS requires greater user training than TLS, as the images must meet all of the aforementioned requirements (good focus, overlapping on all sides, invariant lighting, equal distance from object) for generation of a quality 3D model.

Fig. 6- Showing the poor quality of the model generated with varying light intensities using SFM/MVS

3.3 Evaluation and comparison of reconnaissance techniques

One of the immediate advantages of using TLS and SFM/MVS relative to traditional reconnaissance methods for structural reconnaissance is the generation of a 3D model of the structure. This model provides detailed damage documentation with limited visual gaps and can be used in conjunction with other layers of reconnaissance data to aid in the validation of detailed structural analysis models. Furthermore, the 3D damage documentation models created allows for 3D visualization of structural damage that cannot be seen using conventional means, providing the chance for better understanding of structural performance. However, there are pros and cons to each approach. In terms of data collection, TLS can capture large amounts of field data with millimeter accuracy covering a relatively large area (accuracy decreases at the network (global level) but still mm accuracy is achieved at the relative level within a small area). While SFM/MVS cannot cover large areas with a similar level of accuracy without significant photographic and computational effort, and accurate survey control is required to achieve those higher accuracies. On the contrary, SFM/MVS can provide more detailed models than TLS for a specific, relatively limited region or element (e.g. column or a beam-column joint). Also, TLS models are calibrated so the point cloud already has the correct scale, while for SFM/MVS measurements are required to provide scale for the model generated. This can increase the processing time for SFM/MVS, where survey control is preferred to achieve high accuracy.

The relative performance of both reconnaissance techniques was evaluated based on their ability to capture damage in the case-study building as well as the efficiency with which the data was collected and post-processed. Time consumed in post-processing was determined based on a machine with an Intel® Core™ i7-7700 CPU processor, 16GB RAM and Intel® HD Graphics 630 video card. A summary of the differences found regarding data collection, transfer, and post-processing while utilizing different equipment for both techniques is found in Table 2, where the table mainly compares the required resources (e.g. personnel, equipment and time-on-site) that were required to successfully document the structural damage for the case study building using the different techniques. To compare the ability to capture damage and the level of details captured using each technique, a single column from Pier 3 (in which the cracks were measured and mapped prior to scanning) was used for the comparison as shown in Fig. 7. Note that the point clouds generated using the TLS's have been coupled with panoramic images as shown in Fig. 7 to enhance the visualization of cracking. Results from both TLS's showed that TLS's could detect 2 mm crack widths as shown in Fig. 7b and Fig.7d. Even though one scanner had almost half the capabilities of the other, both were able to detect cracks with widths about 2 mm. Both scanners were able to capture this crack width because the distance from the damaged regions to the scanners was relatively short (approximately 2 m). The highest level of detail achieved was using close-range SFM, where cracks with widths down to 0.65 mm were detected as shown in Fig. 7f.

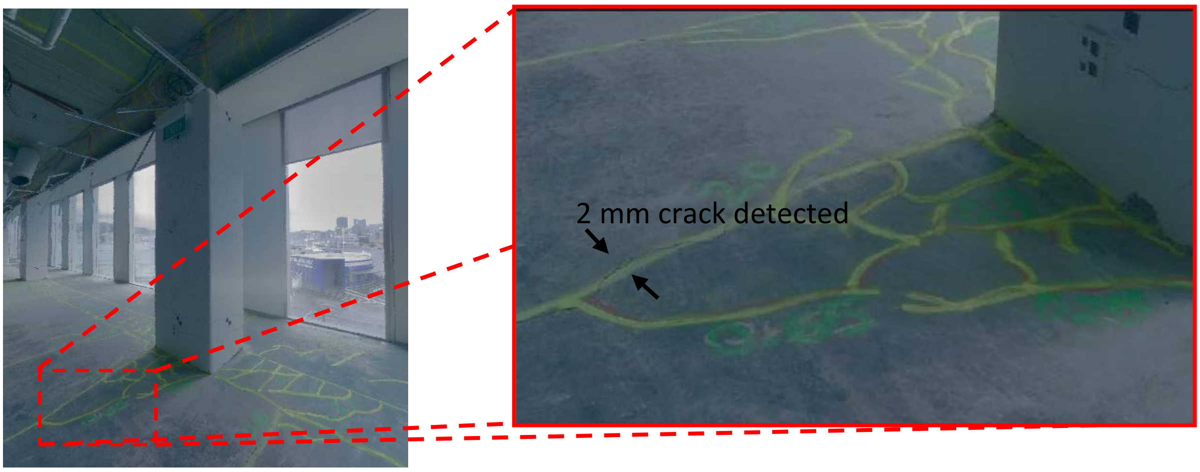

(a) Scanned column using the BLK360 scanner (b) Damage data collected using BLK360 scanner

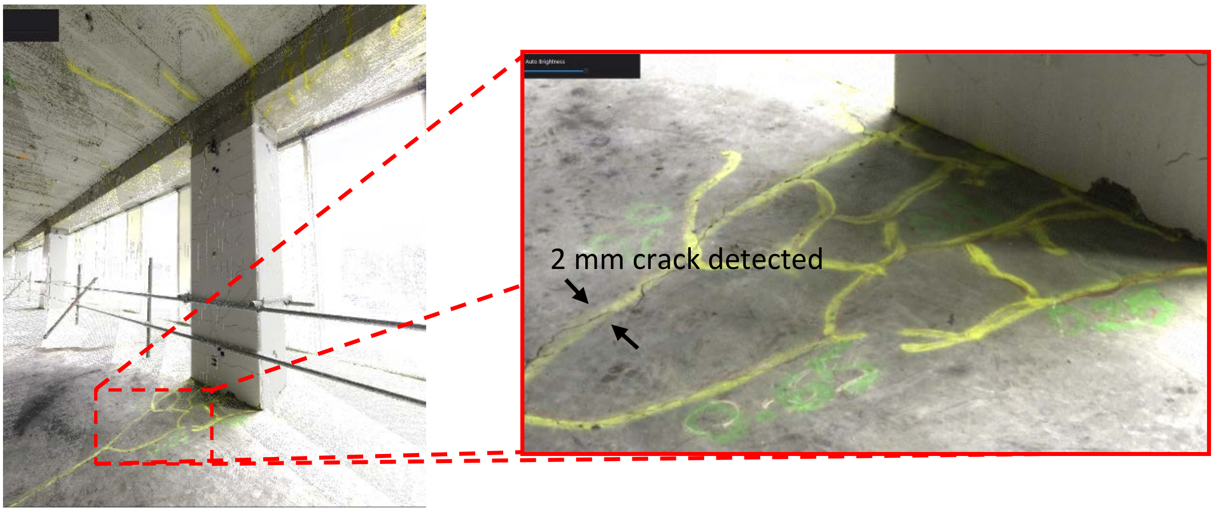

(c) Scanned column using RTC360 scanner (d) Damage data collected using RTC360 scanner

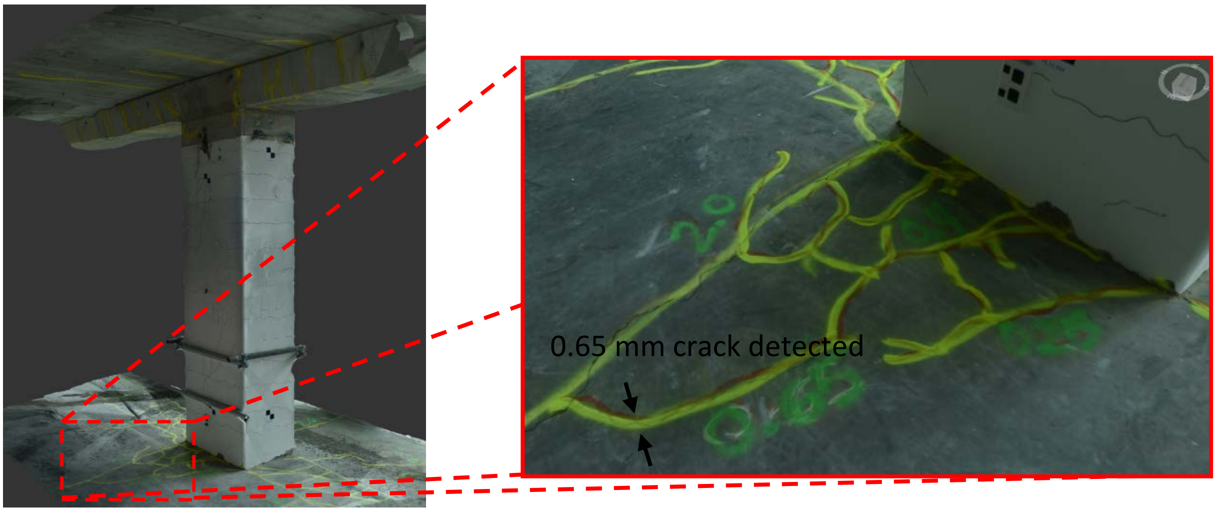

(e) Scanned column using SFM (f) Damage data collected using SFM

Fig. 7- shows an example of the difference in the level of detail in techniques used

The ability to detect cracks of widths reaching below 1 mm allows for assessing different damage categories utilizing crack widths as an indication. For example, according to the Japanese Guideline for Post-earthquake Damage Evaluation and Rehabilitation [15], cracks with widths of approximately 2 mm or larger indicate significant damage to the structure. All three methods were able to detect these crack widths, which suggest all three methods are viable reconnaissance techniques to use if the purpose of the investigation is to determine structural safety or residual capacity. The Japanese Guideline also states that cracks with widths less than 1 mm are indicative of moderate plastic strain demands within the structure. SFM/MVS was the only method trialled that was capable of resolving cracks at this width. The crack widths detected by SFM/MVS (0.4 - 0.65) mm, however, are approaching the smallest width that current products can be used to repair with epoxy injection [16]. As such, SFM/MVS is better suited for determining extent of repairs for cost estimation purposes than the TLS's trialled in this study. It should also be noted that in several cases fine cracks (<1 mm) were filled with dust and were not visible without surface cleaning. However, these cracks were generally outside the detectable range for each reconnaissance type. Finally, the amount of details captured relative to the time consumed is very efficient, and this would have never been achieved using traditional reconnaissance methods.

Table 2 – Comparison of equipment's used in both techniques

	Laser scanning		**SFM/MVS**
	Leica BLK360	**Leica RTC360**	
Captured area	Entire structure	Entire structure	Column regions
Equipment's and Personnel required	Three scanners handled by two people	One scanner handled by one person	One camera used by one person to take images
Time required to collect data from one pier in one floor (Fig.1)	Approximately one and half hours using three scanners (3 man-hours)	Approximately three hours using one scanner (3 man-hours)	Approximately two hours with an average of 65 images per column (2 man-hours)
Data storage and transfer	Data stored on the device's internal memory and transfer took a week relying on Wi-Fi	Data storage and transfer was using a memory stick. And data transfer took almost 8 hours	Data stored and transferred via SD-cards. Transfer took a few hours
Portability	Scanner size is small (165 mm tall x 100 mm dia.), and is light (1 kg)	Scanner size is (120 mm x 240 mm x 230 mm) and weights (5.35 kg)	Cameras are typically used by the reconnaissance teams and are very easy to handle
Post-processing	Time to register the scans was roughly 12-15 days	On-site registration was performed reducing the post-processing time to almost 2.5 days	Each column region took approximately 4 hours to generate the 3D model.

4. Conclusion

The potential application of two data collection state-of-the-art techniques (TLS and SFM/MVS) in post-earthquake structural reconnaissance was investigated, where a comparison of the relative performance in terms of capabilities and limitations of each system in capturing structural damage was performed. The investigation included aspects such as the ability of the different resolution cameras and point clouds of each platform to record cracking, and compared the difference in time-on-site and post-processing for different levels of performance with respect to damage detection. The investigation showed that TLS and SFM/MVS have good merits for capturing structural damage and aiding decision-making post an earthquake event when compared to traditional methods. For example, the level of details reached using SFM/MVS technique to capture cracks with widths less than 1 mm which could aid engineers identify the proper repair methodology for repairable damage. Furthermore, cracks with widths greater than 2 mm were identified by both techniques, which could aid in the decision-making regarding structural integrity post an earthquake. Also, using presented techniques provides a high-resolution 3D model as a digital archive available for further investigation and analysis long after the structure has been demolished. Both techniques could be used together utilizing the high accuracy of TLS to constrain SFM/MSV data, and utilizing the SFM/MVS to fill in the gaps and provide more details for areas of interest. Finally, the amount of details captured relative to the time consumed is very efficient, and such a level of detail in documentation would have never been achieved using traditional reconnaissance methods. Those techniques would have consumed significantly more time and resources to achieve such level of detail for the entire structure, which are not feasible in reconnaissance applications where work must be completed efficiently.

5. Acknowledgments

This investigation is supported by Building Research Association of New Zealand (BRANZ) under Grant No. LR12151 and the University of Auckland. Thanks goes to CentrePort for giving access to the building studied, University of Canterbury post-doctoral fellow Andrew Stolte for his help collecting the data and the Natural Hazards Engineering Research Infrastructure (NHERI) Rapid Facility, sponsored by the National Science Foundation (CMMI-1611820) for providing the BLK360 scanners.

6. References

[1] M. J. Olsen and R. Kayen (2012): Post-earthquake and tsunami 3D laser scanning forensic investigations. Proceedings of the Sixth Congress on Forensic Engineering, 477–486.
[2] R. Langridge, D. Townsend, T. McMorran, C. Anderson, and D. Moroder (2018): Land damage and natural hazards in the Mt Lyford Village area following the 2016 Kaikōura earthquake. GNS Science Consultancy Report 2017/227.
[3] M. J. Olsen and D. T. Gillins (2015): How Can Geomatics Technologies Benefit Geotechnical Studies. 6th International Conference on Earthquake Geotechnical Engineering, Christchurch, New Zealand.
[4] K. M. Mosalam, S. M. Takhirov, and S. Park (2014): Applications of laser scanning to structures in laboratory tests and field surveys. *Struct. Control Health Monit.*, **21**, 115–134. doi: 10.1002/stc.1565.
[5] Earthquake Engineering Research Institute (2004): Learning from Earthquakes Program: A Brief Synopsis of Major Contributions.
[6] Earthquake Engineering Research Institute (1996): *Post-earthquake investigation field guide: learning from earthquake*. Oakland, CA: EERI.
[7] M. J. Olsen, K. F. Cheung, Y. Yamazaki, S. Butcher, M. Garlock, S. Yim, S. McGarity, I. Robertson, L. Burgos, and Y. L. Young (2016): Damage Assessment of the 2010 Chile Earthquake and Tsunami Using Terrestrial Laser Scanning. Earthquake Spectra, **28**, 179–197. doi: 10.1193/1.4000021.
[8] B. Bradley, M. Comerio, M. Cubrinovski, S. Dellow, D. Dizhur, K. Elwood, M. Giaretton, R. Green, N. Horspool, M. Hughes, J. Ingham, L. Johnson, C. Massey, E. Seville, G. Simkin, J. Stevenson, R. Wilson, and L. Wotherspoon (2017): M7.8 Kaikoura, New Zealand Earthquake on November 14, 2016. QuakeCoRE-GEER-EER.
[9] R. S. Henry, D. Dizhur, K. J. Elwood, J. Hare, and D. Brunsdon (2017): Damage to Concrete Buildings With Precast Floors During The 2016 Kaikoura Earthquake. *NZSEE*, **50** (2), 174–186.
[10] D. F. Laefer, M. Fitzgerald, E. M. Maloney, D. Coyne, D. Lennon, and S. W. Morrish (2009): Lateral Image Degradation in Terrestrial Laser Scanning. *Struct. Eng. Int.*, **19** (2), 184–189. doi: 10.2749/101686609788220196.
[11] N. Micheletti, J. H. Chandler, and S. N. Lane (2015): Investigating the geomorphological potential of freely available and accessible Structure-from-Motion photogrammetry using a smartphone. *Earth Surf. Process. Landf.*, **40** (4), 473–486. doi: 10.1002/esp.3648.
[12] Leica-Geosystems (2019): Leica Cyclone Technical Specifications.
[13] CloudCompare (2019): CloudCompare (version 2.11) [GPL software].
[14] Autodesk (2019): Autodesk ReCap Photo Getting Started Guide.
[15] The Japan Building Disaster Prevention Association (1991, revised in 2001 and 2015): *Guideline for Post-earthquake Damage Evaluation and Rehabilitation*.
[16] Sika Australia Pty Limited (2009): Sika Crack Injection System.

